

DOI 10.37943/13PQRV7503

Dinara Kaibassova

PhD, Acting Associate Professor of the Department of Information and Computing Systems
dindgin@mail.ru, orcid.org/0000-0002-8410-7758
Abylkas Saginov Karagandy Technical University, Kazakhstan

Asset Kabdiyev

Master's student of the Department of Information and Computing Systems
assetkabdiyev@gmail.com, orcid.org/0000-0002-2658-9824
Abylkas Saginov Karagandy Technical University, Kazakhstan

PERFORMANCE COMPARISON OF NEURAL NETWORKS IN GRAVITATIONAL LENSING DETECTION

Abstract. A gravitational lens is a distribution of matter, such as dark matter halos, galaxies, or quasars, between a distant light source and an observer that can bend the light from the source as the light travels toward the observer. Nowadays, it is slightly complicated to identify gravitational lenses without powerful computing devices and groups of scientists working together. In addition, future surveys will have orders of magnitude more data and more lenses to find. With up-to-date algorithms such as neural networks, detecting and classifying them for a single human being will be possible. The neural networks described in this paper make the first steps in that direction. The primary purpose of this work was to develop three different neural networks and determine which one could detect gravitational lensing more quickly and precisely. For training, testing, and validation we used a dataset of 2000 images. Half of these images were downloaded from Bologna Lens Factory, a database of simulated gravitational lenses based on galaxies lensed by galaxies (i.e., no clusters and no quasars). We simulated the second half of the images using Python-based code to simulate mock strong lensed galaxies. We used Python-based code to mock strong lensing with different source parameters. Next, we built three types of artificial neural networks and compared their efficiency. Firstly, we developed a fully convolutional neural network (CNN) and a fully connected neural network (FCNN). The third neural network was a combination of these two approaches. In this algorithm, the FCNN layer replaced the last layer of CNN. Next, we compared the learning rates of these algorithms and applied all neural networks to validation images. As a result of the study, we determined which of the developed neural networks fit better for searching gravitational lenses.

Keywords: cosmology, gravitational field, Dark Matter, gravitational lensing, machine learning, image classification, fully connected neural networks, convolutional neural networks

Introduction

Gravitational lensing occurs when the gravity of a massive object causes the deflection of electromagnetic radiation from a distant object. This phenomenon can be seen as a distortion in the light from a faraway galaxy, caused by the gravitational pull of a black hole or galaxy cluster, similar to the way a traditional lens works (as shown in Figure 1).

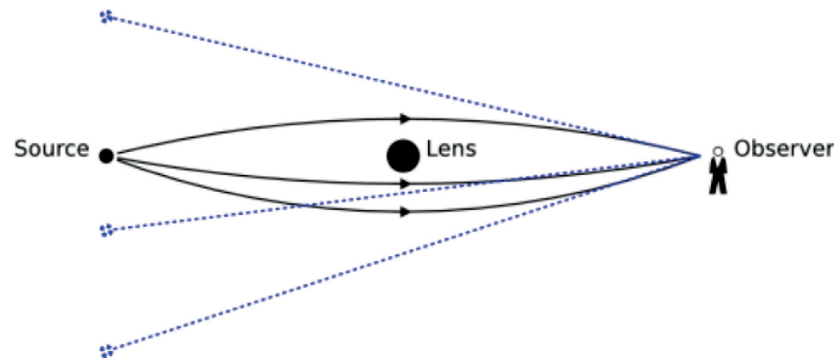


Figure 1. Gravitational lensing

Gravitational lensing now serves as a powerful astrophysical tool to test GR, study distant objects, the distribution of dark matter and the large-scale structure of the universe, relic radiation and even the discovery of planets [1]. One of the new directions in gravitational lensing research is considering plasmas [2]. When calculating and analyzing the effects of gravitational lensing, it is usually assumed that light propagates in a vacuum. However, the cosmic medium is filled with interstellar gas, which is in an ionized state, i.e., actual light rays from the source to the observer propagate through plasma. In its presence, the beams' deflection angles differ from a vacuum's case.

Until now, the most widely used method of searching for lenses in image reviews has been the visual inspection of candidates selected by luminosity and color. However, working with such large amounts of data would only be practical for a visual inspection approach in the future. In addition, human inspection methods' effectiveness and detection of error are challenging to quantify rigorously. Consequently, automatic ways of analyzing data will be crucial for the study of dark matter substructures in the future. Machine learning, particularly deep learning, would be ideal for this task. Currently, convolutional neural networks (CNN), fully connected neural networks (FCNN) or a combination of these two methods can be considered the primary candidates for completing this task. We built all these neural works in our work and chose the most effective one.

Literature Review

The solar eclipse of May 29, 1919 provided the first evidence to support the general theory of relativity, and it also marked the first observed occurrence of gravitational lensing. During this eclipse, the sun's gravitational field caused the starlight to bend slightly [3]. However, under optimal conditions, a lens with a sufficiently high mass density can greatly magnify both an image and its background source. This is known as strong lensing. To understand this phenomenon, we need to consider how light travels from the true source to the observed image. Unlike traditional optics, where there is a single focal point, strong lensing occurs along critical lines, which can magnify the image to infinity. When these critical lines are projected onto the source plane, they form caustics, which depend on the distribution of matter in the lens and the distance between the source and the lens. The location of the background source with respect to these caustics determines the magnification and position of the resulting images [4].

The strong gravitational lensing of galaxies provides valuable information for both astrophysics and cosmology. To date, we have detected several hundred strong lenses between galaxies through diverse searches in photometric and spectroscopic surveys [5]. This sample has been used to learn about the masses and density profiles of galaxies, the population of dark subgalaxies, cosmological parameters, the high-redshift luminosity function [6], and

the characteristics of high-redshift sources [7]. However, the limited number of strong lenses available for analysis is a significant constraint for many of these studies.

Current and future surveys of the wide and deep sky offer improved depth, area, and resolution over existing data and could result in a considerable increase in the number of known strong lenses on galactic scales [8]. A larger sample of strong lenses could also allow for the exploration of smaller lens masses, higher magnitudes, and fainter sources. As a result, it would be possible to investigate trends in the luminosity and redshift properties of lenses and sources. By examining galaxy mass-to-light ratios, dark matter distribution in galaxies, and the population of dark substructures, we could gain tighter constraints on the nature of dark matter, the initial mass function, and the physics of galaxy formation than what is currently possible [9].

In the past, strong gravitational lenses have been discovered by chance during the human analysis of data. However, a systematic search by experts would be too time-consuming for future large-scale research, unless citizen scientists get involved. For instance, the Euclid mission [10] and the Large Synoptic Survey Telescope are expected to uncover over 105 strong lenses among 109 objects. Similarly, the SKA survey is expected to detect a similar number of strong lenses. Therefore, there is a pressing need to develop efficient automated methods for discovering gravitational lenses [11]. Machine learning appears to be the only viable option to human visual inspection for this task. Several groundbreaking works have already demonstrated that ML techniques can effectively find strong lenses in some of the most successful current sky surveys. In fact, the Strong Gravitational Lens Finding Challenge competition compared several lens-finding methods, showing that ML methods perform just as well as human inspection or other traditional methods but with much faster classification rates [12]. As a result, ML methods have found thousands of new lens candidates, quickly catching up with the total number of gravitational lenses discovered by traditional methods over decades. Deep neural networks excel at image recognition, making them ideal for this task.

Neural networks, which are computational systems inspired by the structure of the human brain, are designed to recognize patterns. They consist of three layers: an input layer, a hidden layer, and an output layer. These layers consist of interconnected nodes (artificial neurons) that perform calculations. The first neural network method [13] was trained to identify luminous red galaxy lenses with Einstein radii ≥ 1.4 arcsec and was applied specifically to the kilo-degree survey [14] for redshifts of lensing galaxies $z \leq 0.4$. Another paper [15] published shortly after described the use of deep residual networks (a newer version of CNN) called CMU DeepLens to find strong galactic lenses. The researchers discovered that their method was easier to train and provided accurate results when tested on 20,000 simulated LSST-like images. However, they observed that their method did not show a significant improvement over the method used in previous research despite being more complex, owing to limitations in their modeling.

In a study by Jacobs et al. (2017) [16], four different convolutional neural networks (CNNs) were trained using two different methods, and all networks achieved over 90% accuracy in detecting targets. Several CNNs were tested by another group [17] and found that even simple architectures could achieve high accuracy in their results, indicating that complexity was not always necessary for good performance. However, both studies acknowledged that their accuracy may be limited by the simplicity of their models. CNNs have also been used to analyze images and accurately estimate lensing parameters much faster than previous methods. Hezaveh et al. (2017) [18] created a network capable of achieving parameters ten million times faster, although it is currently limited to a certain density profile. Despite this limitation, CNNs have demonstrated the ability to significantly reduce the time needed to complete such tasks without introducing significant uncertainty, as shown in Levasseur et al. (2017) [19].

Since then, there have been several other scientific works that have applied ML methods to detect gravitational lensing in astronomical images, including Davies et al. (2019) [20] and Wilde J. et al. (2022) [21] research studies. These studies have improved gravitational lens detection using CNNs by using larger and more diverse datasets, more advanced architectures and techniques, and new approaches for combining CNNs with other image analysis techniques. Neural networks can be considered a powerful tool for detecting and analyzing gravitational lenses in astronomical images and may help to improve our understanding of the distribution and properties of dark matter in the universe.

Purpose and Objectives of Research

The aim of the research is to select the most effective neural network among commonly used deep learning methods for detecting gravitational lensing. To achieve this goal, the following tasks should be solved in the paper: select and prepare the proper dataset of gravitational lenses; build three different types of artificial neural networks for detecting gravitational lensing; choose optimal batch size, a number of epochs, optimizer and criterion functions; compare all neural networks' loss graphs and apply them to validation images; based on their learning rate, total loss function and accuracy, select the most fitting one. We also aim to identify effective features and parameters for each neural network architecture, and to compare the generalizability of the different models to new datasets. In addition, we plan to investigate the interpretability of the neural network models and identify the sources of errors and limitations of each architecture. This will provide a comprehensive understanding of the strengths and weaknesses of different neural network models in gravitational lensing detection, and can guide the development of more effective models for future research.

Datasets and Algorithms Description

We used simulated gravitational lens images to train our neural networks, which were obtained from the Bologna Lens Factory. These images were created based on the Millennium project [22], a cosmological N-body simulation that generated a catalogue of dark matter halos and galaxies within a light cone. This catalogue is publicly available and widely used by researchers to study various aspects of the universe, including the evolution of the galaxy luminosity function, clustering of galaxies, and formation of massive galaxy clusters [23]. Our dataset was based on a 1.6 sq.deg. light cone extending out to redshift $z = 6$, and the halos in the catalogue were characterized by their total mass, size, and half-mass radius. The catalogue also included subhalos of larger halos, and the halos were populated with galaxies based on their merger history using the semi-analytic model (SAM). To generate the lensing images, the halo catalogue was read into the GLAMER lensing code [24], which performed all the necessary ray tracing. Within this code, a Navarro, Frenk & White (NFW) profile was fit to the three parameters mentioned above to represent the dark matter component of the lens. Examples of gravitational lenses from the Bologna Lens Factory can be seen in Figure 2.

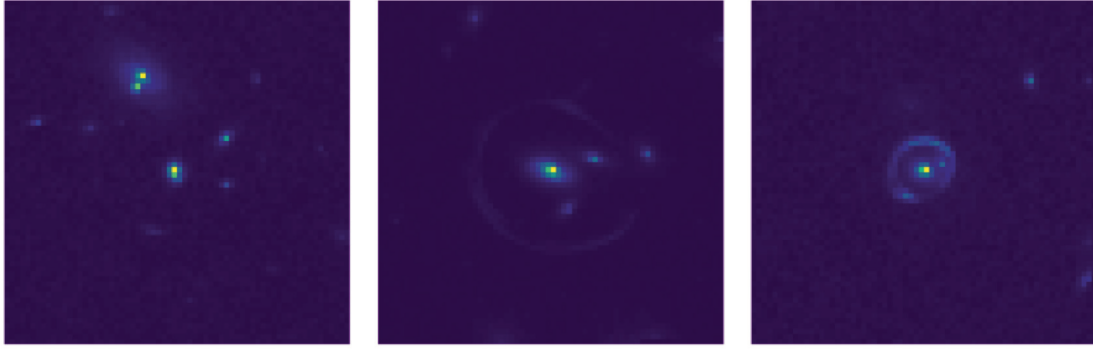


Figure 2. Examples of gravitational lenses from the Bologna Lens factory

The second half of the images were simulated by using Python-based code to simulate mock strong lensed galaxies. Initially, a two-dimensional Sersic profile was set. caustic curve. We began by examining the singular isothermal ellipsoidal lens, where the ellipticity falls within the range of $0 \leq \epsilon < 1/5$. The ellipticity value must satisfy the condition that the surface mass density projected onto the lens plane is non-negative throughout. This condition restricts the ellipticity value to be less than 1. Additionally, the density contours must be convex, which is reasonable for an isolated relaxed system, further constraining the ellipticity value to be less than $1/5$. The lens equation is expressed as:

$$\beta_1 = \theta_1 - \frac{(1-\epsilon)\theta_1}{\sqrt{(1-\epsilon)\theta_1^2 + (1+\epsilon)\theta_2^2}}, \quad (1)$$

$$\beta_2 = \theta_2 - \frac{(1+\epsilon)\theta_2}{\sqrt{(1-\epsilon)\theta_1^2 + (1+\epsilon)\theta_2^2}}, \quad (2)$$

where $\boldsymbol{\beta} = (\beta_1, \beta_2)$ and $\boldsymbol{\theta} = (\theta_1, \theta_2)$ denote the positions of the source and images, respectively. For simplicity, we introduce variables as $x \equiv \sqrt{1-\epsilon}\theta_1$, $y \equiv \sqrt{1+\epsilon}\theta_2$, $a \equiv \sqrt{1-\epsilon}\beta_1$ and $b \equiv \sqrt{1+\epsilon}\beta_2$, so that the lens equation can be rewritten as:

$$a = x \left(1 - \frac{1-\epsilon}{\sqrt{x^2 + y^2}} \right), \quad (3)$$

$$b = y \left(1 - \frac{1+\epsilon}{\sqrt{x^2 + y^2}} \right), \quad (4)$$

Here, we consider off-axis sources ($a \neq 0$ and $b \neq 0$). In this case, Eqs. (3) and (4) show $x \neq 0$ and $y \neq 0$. Eliminating $\sqrt{x^2 + y^2}$ from Eqs. (3) and (4), we obtain as:

$$y = \frac{(1-\epsilon)bx}{(1+\epsilon)a - 2\epsilon x}, \quad (5)$$

The inner and outer caustics are given by:

$$\left(\frac{a^2}{4\epsilon^2} + \frac{b^2}{4\epsilon^2} - 1 \right)^3 + 27 \left(\frac{a^2}{4\epsilon^2} \right) \left(\frac{b^2}{4\epsilon^2} \right) = 0, \quad (6)$$

And the inner caustic given by Eq. (6) is parameterized as:

$$a = 2\epsilon \cos^3 t, \quad (7)$$

$$b = 2\epsilon \sin^3 t, \quad (8)$$

where $t \in [0, 2\pi)$. Then, the caustic curve was plotted on the source plane (in red) along with random source coordinates (in green) using randomly set parameters (Figure 3).

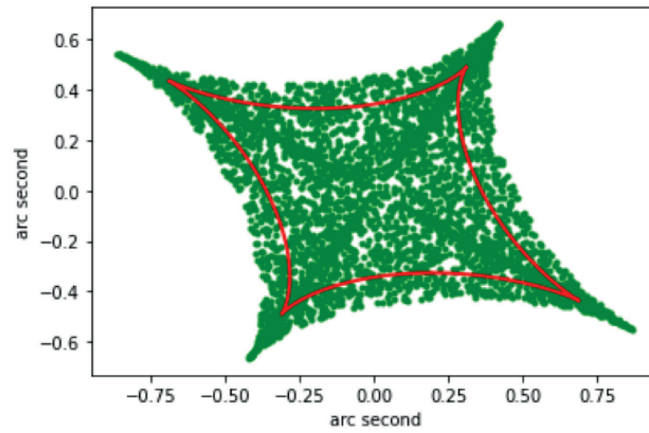


Figure 3. Caustic on the source plane and random source coordinates (green).

The lens potential is modified by adding a simulated Gaussian random field (GRF) potential that follows a power-law power spectrum given by:

$$P^{\delta\psi}(k) = \mathcal{A} \cdot k^{-\beta}, \quad (9)$$

The amplitude \mathcal{A} in the power law is determined using Parseval's theorem, which relates the variance of the GRF potential fluctuations inside the image, denoted by σ_{fluct}^2 , to the normalization factor:

$$\mathcal{A} = \frac{\sigma_{\text{fluct}}^2 N_{\text{pix}}^2}{2 \sum k^{-\beta}}, \quad (10)$$

To calculate the sum, we consider all possible values of k , which is the magnitude of the wave vector in Fourier space and is calculated as the square root of the sum of squares of k_x and k_y . In our simulations, we use a Fourier grid of size 121x121. In this case, a DFT of one random realization of the above power spectrum leads to a GRF potential field with a variance of σ_{fluct}^2 . Using these parameters, we can generate a random realization of the GRF potential field. We plot an example of the GRF potential field created by randomly chosen parameters in Figure 4.

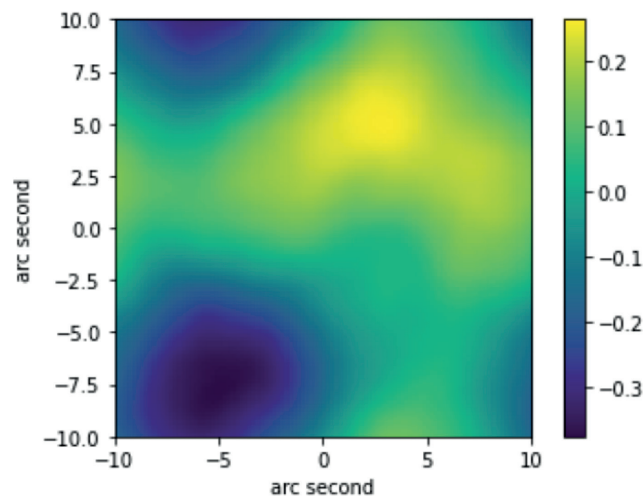


Figure 4. Gaussian random field

After setting proper lens plane parameters, Sersic source parameters and parameters for the blob sub-structures in the source, we were ready to simulate gravitational lenses and their sources (Figure 5).

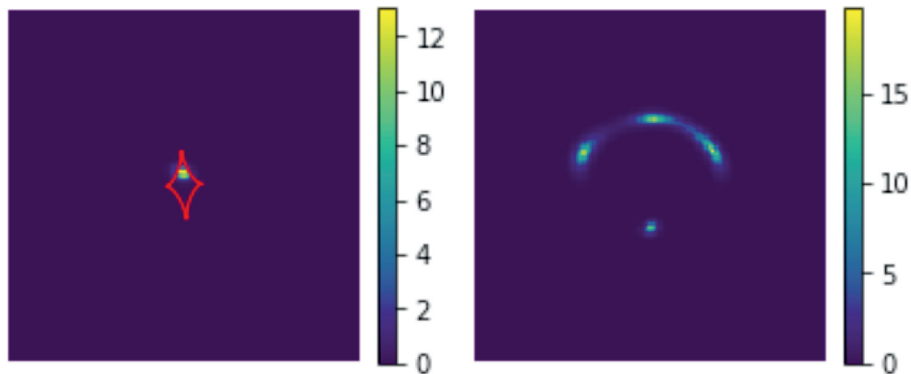


Figure 5. Example of a simulated gravitational lens and their source

We used Python programming language and worked in the Google Colab environment to solve the following problems. First, to start processing the lensing images we will be using to train our CNN, we downloaded all datasets in special astronomical image format. The total size of the dataset was 2000 images. The training set had 1050 images, and one lens and not lens images were used for validation Fig. 6. In the beginning, we started to make our neural networks by importing the necessary libraries: PIL, Random, Glob etc. In addition to Matplotlib and Numpy, we used Pytorch for all the deep-learning calculations. We then imported Torchvision, which contains a lot of popular data sets and models that are useful for measuring the performance of our custom model against the previous state of the art. All data should be correctly prepared before we would start to train it. It was transformed into tensors, and then we defined a class that helped us divide data and select it randomly. The data were divided into batches; the batch size was 32 units. To measure total error and loss we used a criterion that measures the Binary Cross Entropy between the target and the input probabilities (BCELoss). The unreduced loss can be described as:

$$l(x, y) = L = \{l_1, \dots, l_N\}^T, \quad (11)$$

$$l_n = -w_n [y_n \cdot \log x_n + (1 - y_n) \cdot \log(1 - x_n)]. \quad (12)$$

Accuracy score measured the number of correct predictions made by a model in relation to the total number of predictions made.

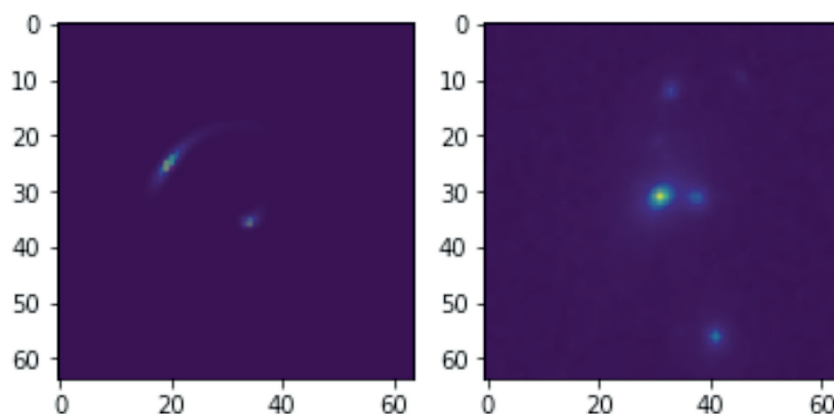


Figure 6. Validation images

Fully Convolutional Neural Network

After preparing the data, we constructed fully CNN by using Conv2D convolution layers. We had three channels but were free to change this for other types of images, and our image sizes were 64 by 64. After adding the first convolutional layer, we started with the number of channels coming in and then put the number of channels or the number of layers that we want out. The number of feature maps had a kernel size of 4, strides of 2 and padding of 1. We wanted to end up with a number of feature maps of size 128 by 128. Then we applied batch normalization and ReLU to our feature maps. In the next convolutional layer, we multiplied the output by two for deeper throughout the network, and all other parameters remained the same. The process was iterated 5 times until getting a 1x1x1 tensor layer with an output of numbers ranging from 0 to 1. We chose 30 training epochs, Adam as Optimizer and BCELoss as a criterion and used CUDA as a parallel computing platform. Then, all data were divided into mini-batches. Finally, our neural networks were trained by iterating through these mini-batches in the training set and mini-batches in the testing set. Training started with a very high loss at the beginning, and it's quickly gone down to even less than 0.1 error (Figure 7). Table 1 shows the accuracy of validation images, total error and total accuracy of the testing dataset.

Table 1. Fully CNN's accuracy and error rate

	Testing dataset	Gravitational lens image	Not gravitational lens image
Accuracy	97.9%	98.7%	99.3%
Error	0.0102	0.0032	0.0011

Fully Connected Neural Network

To summarize, fully connected neural networks are neural networks where all neurons in one layer are connected to neurons in the next layer. While not commonly used for image classification, they have the advantage of being structure agnostic. In this study, the model started with a linear regression layer of size 642x642, with the output normalized by one-dimensional batch normalization and applied the ReLU activation function. The model consisted of 7 linear regression layers, with the last layer squeezed to 192x1 for final classification using the Sigmoid function. The final train and test loss values were greater than 1 and 2, respectively, as shown in Figure 8. The validation images were difficult for the network to classify, as shown in Table 2, but the overall accuracy was more than 80%.

Table 2. FCCN's accuracy and error rate

	Testing dataset	Gravitational lens image	Not gravitational lens image
Accuracy	82.5%	55.7%	47.2%
Error	0.394	0.712	0.871

Fully Connected Layer in CNN

Fully connected layers are utilized to allow for more connectivity possibilities and enable updating weights during back-propagation. These layers connect every neuron in one layer to every neuron in the following layer. Our algorithm follows the CNN process, but we modified the last hidden layer from a Conv2D layer to a fully connected output layer, combining an Affine and Non-Linear functions. The flattened layer, which is a one-dimensional layer, provides input data to the fully connected layer. The data from the Flatten layer is first passed through the affine function and then through the non-linear function, which together form one fully

connected or flattened layer. The output from the final hidden layer is fed into the Sigmoid function to create a probability distribution over the set of classes. The final training loss value is close to 0.5, while the test loss value is 0.3 (Figure 9). Table 3 shows the accuracy of validation images, total error, and total accuracy of the testing dataset.

Table 3 CNN with fully connected layer's accuracy and error rate

	Testing dataset	Gravitational lens image	Not gravitational lens image
Accuracy	97.2%	96.8%	99.1%
Error	0.0825	0.0132	0.0076

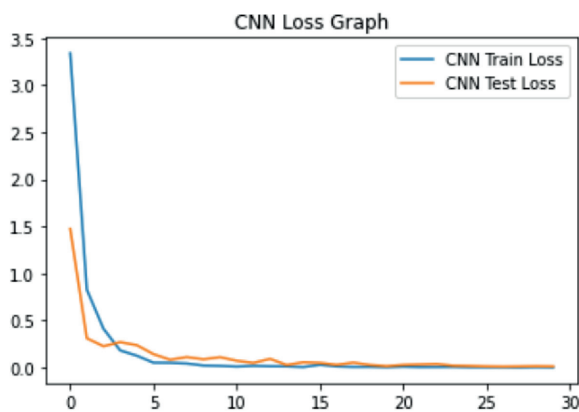


Figure 7. CNN's loss graphs

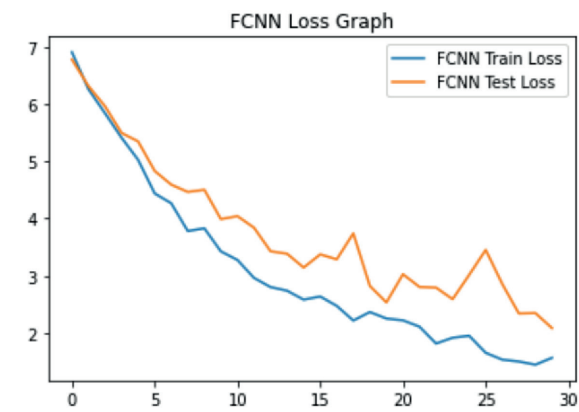


Figure 8. FCNN's loss graphs

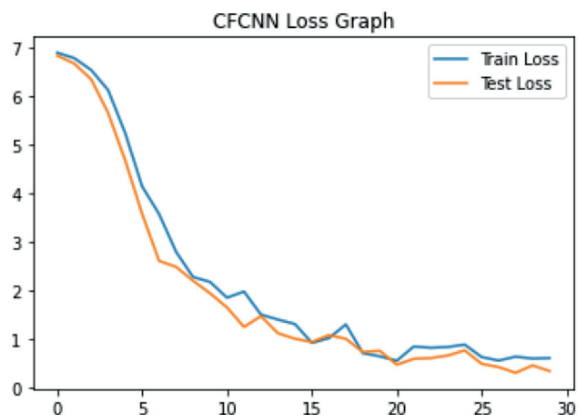


Figure 9. CFCNN's loss graphs

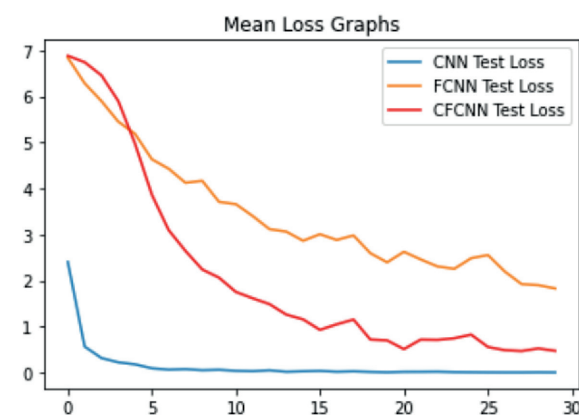


Figure 10. Mean loss graphs

Discussion of Results

All developed deep-learning algorithms have shown the ability to detect gravitational lensing, but not all of them were equally efficient. The least effective compared to other neural networks was a fully connected neural network. This type of network is a good enough classifier, but they aren't good for feature extraction. Before the emergence of CNNs, people usually used FCNN, and the state-of-the-art was to extract explicit features from images and then classify these features. Nowadays, data scientists rarely use this algorithm for image classification; the resulting accuracy and total loss function explain why. More interesting was the comparison of a fully CNN and a CNN with a fully connected layer. Although the CNN with the fully connected layer showed markedly low losses and very high accuracy, the fully connected CNN had a much higher learning rate and slightly better other results. Both

algorithms can successfully detect gravitational lensing images, but fully CNN can do it much faster. The mean loss functions of all three neural networks are shown in Figure 10.

Conclusions

In this scientific paper, we successfully developed and compared three commonly used deep learning algorithms for gravitational lensing detection. Despite the fact that FCNN failed to recognize validation images and had low overall performance, two other neural networks showed the ability to classify gravitational lensing images. In the future, both fully CNN and CNN with the fully connected last layer can be used to find new galaxies or dark matter halos by inspecting potential gravitational lensing images. Of the two, fully CNN is the preferred algorithm because of the faster learning process and less loss. Consequently, this model requires fewer input data to train. Only this model showed no signs of overfitting due to the minimal difference between the training and testing loss values. Other neural networks have problems with generalization because we didn't use a very large dataset, and this is something you might have to deal with if your dataset is limited, like the one we used in our paper.

Based on results, developed fully CNN can be a powerful tool for identifying new gravitational lens candidates, which in turn can lead to the discovery of new galaxies and structures, providing valuable insights into the distribution of matter in the universe, the properties of dark matter, and the nature of dark energy. In future works, we plan to use extended datasets with different types of lenses, try other types of neural networks, and compare their results again.

References

1. Sjur Refsdal. (1964). On the Possibility of Determining Hubble's Parameter and the Masses of Galaxies from the Gravitational Lens Effect, *Monthly Notices of the Royal Astronomical Society*, 128(4), 307-310.
2. Bisnovaty-Kogan G.S., Tsupko O.Yu. (2015). Gravitational lensing in plasmic medium, *Plasma Physics Reports*, 41(7), 562-581.
3. Thomas E. Collett. (2015). The population of galaxy-galaxy strong lenses in forthcoming optical imaging surveys, *Astrophysical Journal* 811: 20.
4. Ellis Richard S. (2010). Gravitational lensing: a unique probe of dark matter and dark energy, *Philosophical Transactions of the Royal Society*, A.368, 970.
5. Barnabè M., Czoske O., Koopmans L.V.E., Treu T. & Bolton A.S. (2011). Two-dimensional kinematics of SLACS lenses – III. Mass structure and dynamics of early-type lens galaxies beyond $z \approx 0.1$, *Monthly Notices of the Royal Astronomical Society*, 415, 2215-2232.
6. Barone-Nugent, R.L., et al. (2015). The impact of strong gravitational lensing on observed Lyman-break galaxy numbers at $4 \leq z \leq 8$ in the GOODS and the XDF blank fields, *Monthly Notices of the Royal Astronomical Society* 450.2, 1224-1236.
7. Collett, Thomas E. (2015). The population of galaxy-galaxy strong lenses in forthcoming optical imaging surveys, *Astrophysical Journal* 811.1, 20.
8. Kuhlen, Michael, Charles R. Keeton, and Piero Madau. (2004). Gravitational lensing statistics in universes dominated by dark energy, *Astrophysical Journal* 601.1: 104.
9. Sonnenfeld, Alessandro, et al. (2013). The SL2S galaxy-scale lens sample. III. Lens models, surface photometry, and stellar masses for the final sample, *Astrophysical Journal* 777.2, 97.
10. Laureijs, Rene, et al. (2011). Euclid definition study report, *arXiv*: 1110.3193: 8.
11. Braun, Robert & Bourke, T & Green, James & Keane, Evan & Wagg, Jeff. (2015). *Advancing Astrophysics with the Square Kilometre Array*, 174.
12. Metcalf, R.B., Meneghetti, M.A.S.S.I.M.O., Avestruz, C., Bellagamba, F., Bom, C.R., Bertin, E., ... & Vernardos, G. (2019). The strong gravitational lens finding challenge. *Astronomy & Astrophysics*, A119, 625.

13. Petrillo, C.E., Tortora, Chatterjee, S., Vernardos, G., Koopmans, L.V.E., Verdoes Kleijn, G., ... & McFarland, J. (2017). Finding strong gravitational lenses in the kilo degree survey with convolutional neural networks. *Monthly Notices of the Royal Astronomical Society*, 472(1), 1129-1150.
14. de Jong, J.T., Verdoes Kleijn, G.A., Kuijken, K.H., & Valentijn, E.A. (2013). The kilo-degree survey. *Experimental Astronomy*, 35(1), 25-44.
15. Lanusse, F., Ma, Q., Li, N., Collett, T., Li, C., Ravanbakhsh, S., ... & Póczos, B. (2018). CMU DeepLens: deep learning for automatic image-based galaxy-galaxy strong lens finding. *Monthly Notices of the Royal Astronomical Society*, 473(3), 3895-3906.
16. Jacobs, C., Glazebrook, K., Collett, T., More, A., & McCarthy, C. (2017). Finding strong lenses in CFHTLS using convolutional neural networks. *Monthly Notices of the Royal Astronomical Society*, 471(1), 167-181.
17. Jaeger-Erben, M., Rückert-John, J., & Schäfer, M. (2017). Soziale Innovationen für nachhaltigen Konsum: Wissenschaftliche Perspektiven, Strategien der Förderung und gelebte Praxis. In *Soziale Innovationen für nachhaltigen Konsum* (pp. 9-21). Springer VS, Wiesbaden.
18. Hezaveh, Y.D., Levasseur, L. P., & Marshall, P.J. (2017). Fast automated analysis of strong gravitational lenses with convolutional neural networks. *Nature*, 548(7669), 555-557.
19. Levasseur, L.P., Hezaveh, Y.D., & Wechsler, R.H. (2017). Uncertainties in parameters estimated with neural networks: Application to strong gravitational lensing. *The Astrophysical Journal Letters*, 850(1), L7.
20. Davies, A., Serjeant, S., & Bromley, J.M. (2019). Using convolutional neural networks to identify gravitational lenses in astronomical images. *Monthly Notices of the Royal Astronomical Society*, 487(4), 5263-5271.
21. Wilde, J., Serjeant, S., Bromley, J. M., Dickinson, H., Koopmans, L.V., & Metcalf, R.B. (2022). Detecting gravitational lenses using machine learning: exploring interpretability and sensitivity to rare lensing configurations. *Monthly Notices of the Royal Astronomical Society*, 512(3), 3464-3479.
22. Overzier, R., Lemson, G., Angulo, R.E., Bertin, E., Blaizot, J., Henriques, B.M.B., ... & White, S.D.M. (2013). The millennium run observatory: first light. *Monthly Notices of the Royal Astronomical Society*, 428(1), 778-803.
23. Glenn, J., Bradford, C.M., Rosolowsky, E., Amini, R., Alatalo, K., Armus, L., ... & Zmuidzinas, J. (2021). Galaxy evolution probe. *Journal of Astronomical Telescopes, Instruments, and Systems*, 7(3), 034004-034004.
24. Petkova, M., Metcalf, R.B., & Giocoli, C. (2014). glamer-ii. multiple-plane gravitational lensing. *Monthly Notices of the Royal Astronomical Society*, 445(2), 1954-1966.